Original Article

The Ability for the Extracellular Production of Iron Oxide Nanoparticles by *Klebsiella pneumoniae* and *Staphylococcus aureus*

Diana Faisal Ali Rasheed[1], Hiro Mohammed Obaid[2]

[1]Department of Microbiology, Azadi Teaching Hospital, Kirkuk Directorate of Health, Kirkuk, Iraq, [2]Department of Medical Laboratory Techniques, College of Health and Medical Technology, Northern Technical University, Kirkuk, Iraq

Abstract

Background: The biological production of nanoparticles is emerging as a possible method for nanoparticle synthesis due to its simplicity and lack of toxicity. Recent research has looked into microorganisms as a potential biofactor for the manufacture of many nanoparticles (NPs). **Objectives:** The aim of this paper is to screen a variety of common bacteria in order to assess the extracellular biosynthetic potential of metallic NPs like iron oxide (Fe_2O_3) NPs **Materials and Methods:** By using *Staphylococcus aureus* and *Klebsiella pneumonia* as possible candidates for the quick synthesis of NPs, ferric nitrate was exploited as a source of Fe_2O_3 NPs. A reduction of aqueous solutions with bacterial cell-free filtrates was used to create Fe_2O_3 NPs. **Results:** Characterization of synthesized NP conducted by UV–Vis spectroscopy and the maximum peak at 407 nm absorbance for *K. pneumoniae* Fe_2O_3 NPs. Also, 408 nm *S. aureus* Fe_2O_3 NPs. **Conclusion:** The ability of the isolated bacteria to synthesize iron oxide NPs in large quantities is demonstrated by the success of the stabilized F_e3O_4 NP synthesis, which was capped by the organic group.

Keywords: Characterization, extracellular, *Klebsiella pneumoniae*, Nanoparticles, organic, *Staphylococcus aureus*

Introduction

Nanotechnology is a multidisciplinary kind of science that covers many areas of scientific techniques, like biomedical, pharmaceutical, agricultural, environmental, materials, general chemistry, general physics, electronics, data sciences, technology, etc.[1-5] Nanoparticles (NPs) are materials with two or more dimensions and a diameter between 1 and 100 nm.[6] Iron oxide NPs are technologically important due to their fascinating magnetic and electrical characteristics. They are employed in the creation of magnetic cores for read/write heads for high-speed digital tapes or disc recording, as well as in magnetic inks and magnetic fluids.[7] Iron oxide NPs can be made using a variety of synthesis techniques, such as the hydrothermal reaction method, the sol–gel process, and chemical coprecipitation, although these nanomaterials often have low homogeneity for particle size.[8] Microorganisms, due to their distinctive qualities, which include the ability to survive in difficult environments and under environmental stress, high metabolic diversity, high substrate specificity, and faster development, as well as benefits including the ability to use them in environments with relatively mild temperature, pH, and pressure. Their proper operation as suitable biocatalysts in two-phase systems composed of water and organic solvents, as well as the primary contributors in environmentally friendly nanofactories for the creation and assembly of nanosized particles containing metal, are of paramount importance.[9-11] In the reduction of metal, several extracellular enzymes can serve as an electron shuttle because they exhibit exceptional redox characteristics. It is also obvious that ions can be reduced to NPs by electron shuttles or other reducing

Access this article online

Quick Response Code:

Website: https://journals.lww.com/mjby

DOI: 10.4103/MJBL.MJBL_1212_23

Address for correspondence: Dr. Diana Faisal Ali Rasheed, Department of Microbiology, Azadi Teaching Hospital, Kirkuk Directorate of Health, Iraq.
E-mail: dianafaisal6@gmail.com

Submission: 15-Aug-2023 **Accepted:** 29-Oct-2023 **Published:** 30-Apr-2026

How to cite this article: Rasheed DFA, Obaid HM. The ability for the extracellular production of iron oxide nanoparticles by *Klebsiella pneumoniae* and *Staphylococcus aureus*. Med J Babylon 2026;23:392-7.

agents, such as hydroquinones produced by microbes.[12] The biologically produced NPs have better enzyme and metal salt properties, as well as stronger catalytic reactivity and a bigger specific surface area.[13] The biological method is a more palatable green alternative that uses less energy and is also environmentally friendly.[14,15] The microbial generation of Fe_2O_3 NPs was examined in the current work. This research suggests the creation of Fe_2O_3 NPs using the bacterial (*Staphylococcus aureus* and *Klebsiella pneumonia*) isolate as a reducing agent.

Materials and Methods

Extracellular synthesis of NPs by using microorganisms

Preparation isolates of bacteria

The isolates came from the Azadi Teaching Hospital's Microbiology Department, where the disease had previously been identified using a Vitek 2 system and biochemical test. *S. aureus* and *K. pneumonia* were two of the isolates that were employed in the production of iron oxide NPs.[16]

Preparation of supernatant solution of bacteria

Pure bacterial isolates were inoculated into 100 mL of sterile Luria Bertani broth for *K. pneumoniae* and nutritional broth media for *S. aureus* under sterile conditions. These media were then incubated at 37°C for 24 h. After the incubation period, the bacterial culture is centrifuged at 6000 rpm for 12 min, after which the cell supernatants are separately collected for each isolate in a sterile 250 mL conical flask for the creation of NPs.[17]

Preparation of iron oxide NP

For biosynthesis, 2 g ferric nitrate $Fe(NO_3)_3$ was dissolved in 40 mL of deionized water using a magnetic stirrer for 30 min. Then, the bacterial culture supernatant (*S. aureus* or *K. pneumoniae*) was mixed with the precursor solution of ferric as a ratio (1:1) by magnetic stirrer for 1 h and another bacterial culture without ferric nitrate was used for control, after which 2 M of sodium hydroxide (NaOH) was added drop-wise. The solution was left for 48 h in the incubator. After incubation, it is washed with water and ethanol and then separated by centrifuge. Then, it dried in the oven with the formation of a fine powder. A Perkin-Elmer Lambda 2 Spectrophotometer was used to conduct UV–Vis spectroscopy (UV–Vis) in the 200–900 nm range to determine the presence of iron oxide NPs.[16,17]

Ethical approval

The study was conducted in accordance with the ethical principles that have their origin in the Declaration of Helsinki. It was carried out with the patient's verbal and analytical approval before the sample was taken. The study protocol, the subject information, and the consent form were reviewed and approved by a local ethics committee according to document number 5186 on October 26, 2022.

Results

Bacterial identification

The microorganisms recovered from plates were fully identified by Colony morphology (hemolysis, pigment, and size) and Gram's stain.

Isolates that grey pigmented, smooth, convex, and hemolytic colonies on blood agar are suspected to be *S. aureus*. These isolates were examined under a light microscope after staining by Gram stain, and the cells appeared as Gram-positive cocci (in grape-like irregular clusters), more purified by biochemical tests (positive result for catalase, coagulase test, and slide coagulase test, and oxidase negative). All the *S. aureus* isolates have the ability to grow on mannitol salt agar and form large, round, creamy-golden colonies surrounded by wide yellow zones and turn the color of the medium from pink to yellow and on Baird–Parker agar *Staphylococci* can reduce tellurite to telluride, which results in dark gray to black, shiny, convex colonies with entire margins and clear zones with

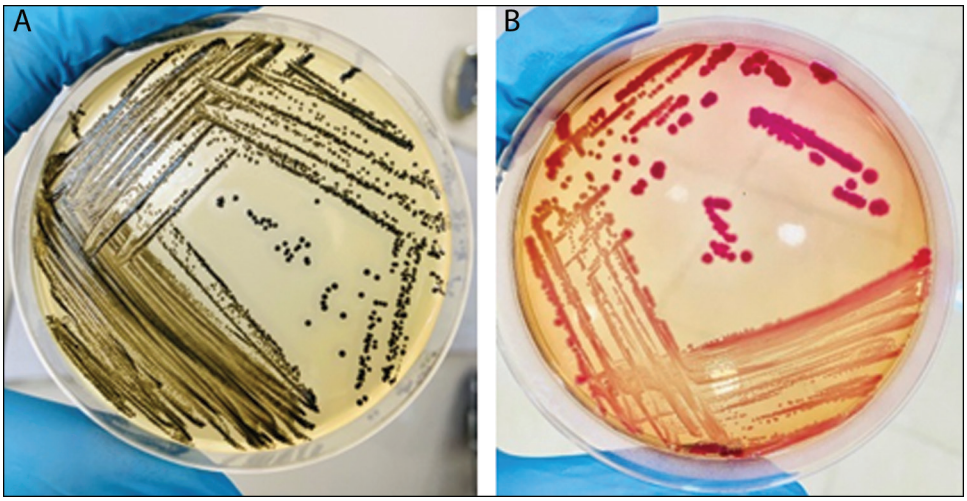

Figure 1: (A) *S. aureus* on Baird–Parker agar and (B) *K. pneumoniae* on MAC agar

or without an opaque zone around the colonies due to the addition of egg yolk, as shown in [Figure 1A].

In a microscopic examination, ×100 power *Klebsiella* isolates showed a distinct capsule when stained with a negative stain. *Klebsiella* reacted negatively with Gram stain, and they showed characteristic red single. Double or short-chain rods. Morphological examination of *K. pneumoniae* isolates grown on MacConkey agar medium gave the pink glamorous colonies with mucus texture due to the ability to lactose fermenting [Figure 1B].

Biosynthesis of iron oxide NPs using bacteria

The synthesis of IONPs by *S. aureus* and *K. pneumoniae* was indicated through the changing color of the reaction from light yellow to red color within 48 h of inoculation, and the color intensity increased with the added drop-wise of (NaOH) due to the reduction in Hassan and Mahmood[18] [Figure 2].

Figure 2: Visual observation of iron oxide NPs formation by color changing from light yellow to red after 48 h

Characterization of Fe_2O_3 NPs

UV–VIS spectroscopy test

The synthesis of Fe_2O_3 NPs accompanied by changes in the color of the broth suspension from light yellow to red confirmed iron oxide NPs production was down by UV–Vis spectroscopy technique. Various suspension concentrations showed different absorption peaks, and the maximum peak at 407 nm absorbance for *K. pneumoniae* Fe_2O_3 NPs, as shown in Figure 3A]. This obtained results near from that reported in the study of Jagathesan and Rajiv.[19] Also, 408 nm *S.aureus* Fe_2O_3 NPs [Figure 3B] were near the documented result for UV–visible absorption.[20]

Characterization by TEM

Transmission electron microscopy was used to characterize the morphology of the produced Fe_2O_3 NPs. The TEM picture [Figure 4A] shows the development of Fe_2O_3-NPs biosynthesized from *K. pneumoniae* with a spherical shape predominantly irregular in shape and an average size of 20–100 nm. The size of Fe_2O_3 NPs from *S.aureus* appears roughly spherical in shape, with a relatively uniform diameter of (30–100 nm), as appears in [Figure 4B].

SEM and EDS characterization

The morphology and elemental makeup of the produced Fe_2O_3 NPs were determined using SEM and EDS analysis. The F_e3O_4 NPs' rodlike shape. The synthetic Fe_2O_3 *K. pneumniae* NPs ranged in size from 36.35 to 49.33 nm, are depicted in Figure 5A. While the size of the synthesized Fe_2O_3 *S. aureus* NPs ranged from 30.37 to 55.87 nm [Figure 5B].

XRD characterization

The rhombohedral crystal system of the synthesized Fe_2O_3 NPs was confirmed by the XRD [Figure 4]. The crystalline size values and structural parameters of Fe_2O_3 NPs synthesized by *K. pneumoniae* show a separated peak at 2θ = 24.1°, 33.1°, 35.5°, 40.8°, 49.5°, 54.0°, 57.3°, 62.6°, 63.9°, 69.5°, 71.9°, and 75.5°, with orientation (012), (104), (110), (113), (024), (116), (122), (214), (300), (208),

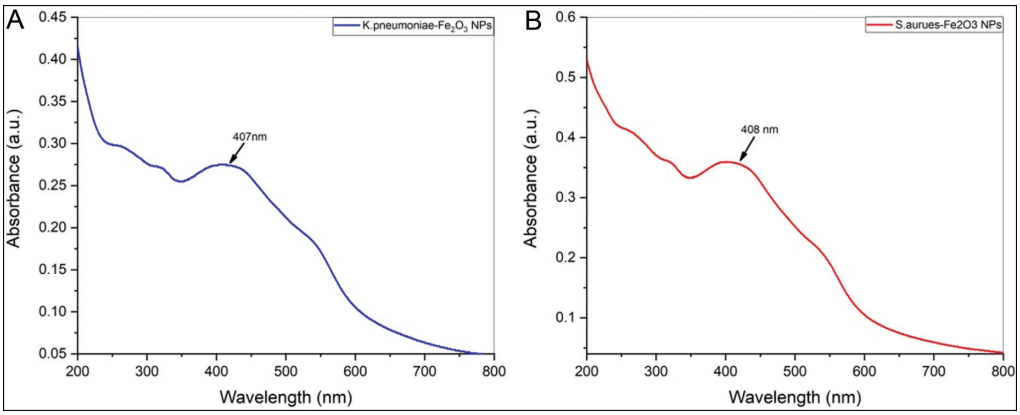

Figure 3: UV–visible spectrophotometer (A) absorbance of Fe_2O_3 *K. pneumoniae* and (B) Absorbance of Fe_2O_3 *S. aureus*

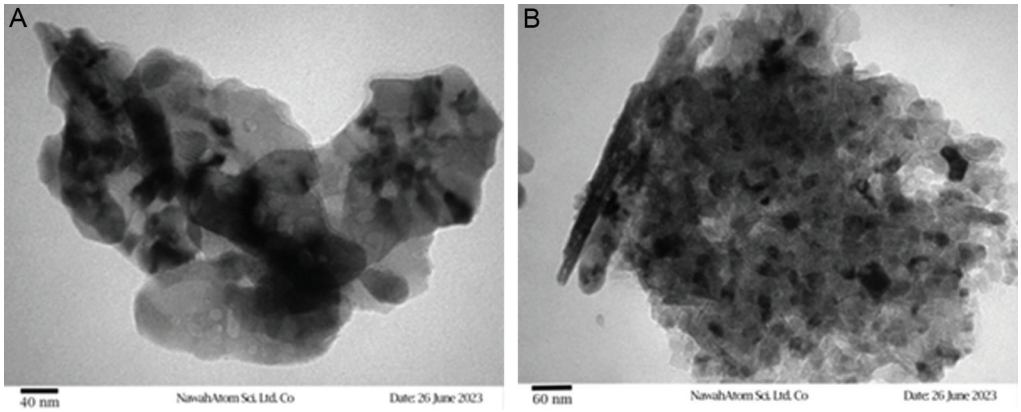

Figure 4: TEM images for synthesized NPs: (A) Fe_2O_3 *K. pneumniae* NPs, (b) Fe_2O_3 *S. aureus* NPs

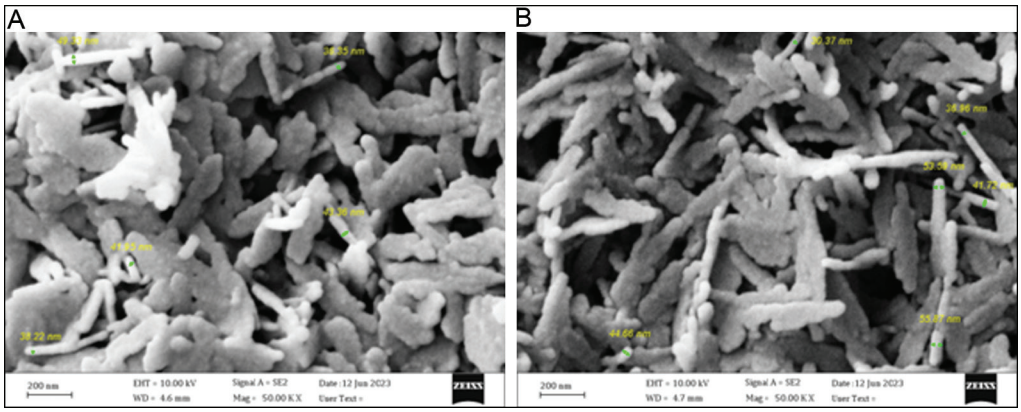

Figure 5: SEM images for synthesized NPs: (A) Fe_2O_3 *K. pneumniae* NPs, (b) Fe_2O_3 *S. aureus* NPs

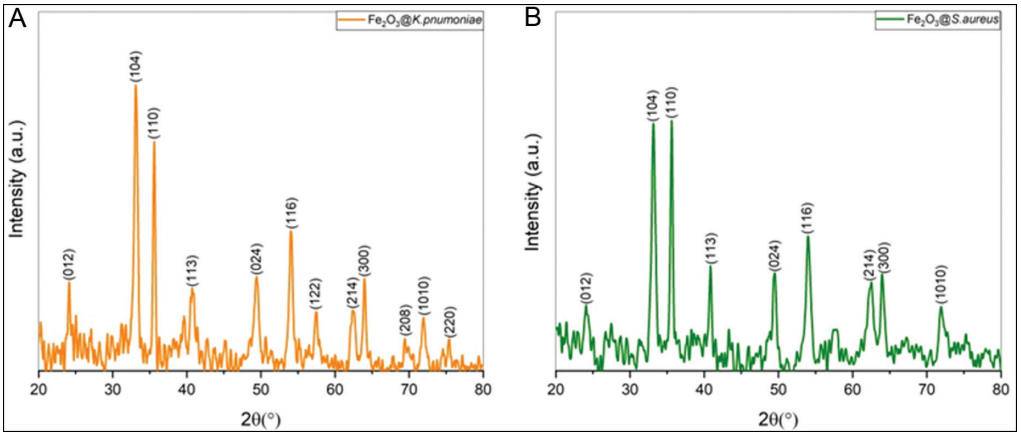

Figure 6: XRD polt: (A) Fe_2O_3 *K. pneumoniae* and (B) Fe_2O_3 *S. aureus*

(1010), and (220). The mentioned peaks are matched with the diffraction data standard of Fe_2O_3 NPs (ICPDS file no. 00-024-0072) [Figure 6A]. At the same time, the crystalline size values and structural parameters of Fe_2O_3 NPs synthesized by *S. aureus* show a separated peak at 2θ = 24.1°, 33.1°, 35.6°, 40.8°, 49.4°, 54.0°, 62.6°, 63.9° and 71.8°, with orientation (012), (104), (110), (113), (024), (116), (214), (300), and (1010). The mentioned peaks are matched with the diffraction data standard of Fe_2O_3 NPs (ICPDS file no. 01-079-1741) [Figure 6B]. These findings were in agreement with the previous studies.[21,22]

Discussion

The preparation route reported here has been successful in providing NPs in which the iron is present exclusively as Fe(II). The alteration in color of the combination is due to the excitation of surface plasmon vibrations in the iron oxide NPs, which is the characteristic property of the

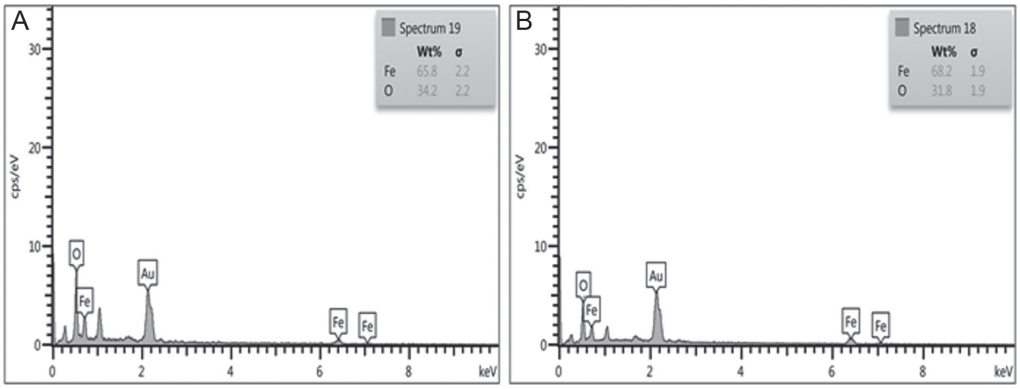

Figure 7: EDX spectrum: (A) Fe_2O_3 *K. pneumniae* NPs and (b) Fe_2O_3 *S. aureus* NPs

NPs. This result agrees with several hypotheses reported that one possible mechanism, the NADH-dependent nitrate reductase, an enzyme secreted by (*S. aureus* and *K. pneumoniae*) is responsible for the reduction of Fe metal in the biosynthesis of iron oxide NPs.[23]

The difference in the shapes and sizes of the synthesized NPs was studied using TEM images. The size of Fe_2O_3 NPs biosynthesized from *K. pneumoniae* at a magnification of 77,500 k× appears spherical shape and predominantly irregular in shape with an average size of 20–100 nm. In the recent study, for Fe_2O_3 NPs from *S. aureus*, the size appears at 29.5 nm with different shapes such as rod, hexagonal, and cubic structures. The measured particle size is consistent with that predicted by the Scherrer equation, which predicts an average particle size of 14 nm. The NPs were generally evenly distributed, while some of them were slightly agglomerated. The small majority of the particles in the TEM pictures were less than 100 nm in size, with the few large particles possibly the result of the agglomeration of smaller particles; our results agree with the previously reported result.[21,24] The size of Fe_2O_3 NPs from *S. aureus* appears roughly spherical in shape, which is also reported.[21,24,25] The measured particle size is consistent with that predicted by the Scherrer equation, which predicts an average particle size of 17 nm.

The morphology and elemental makeup of the produced Fe_2O_3 NPs were determined using SEM and EDS analysis. Pure iron oxide NP production has been verified by EDX analysis. The cleanliness of the particles in this spectrum was examined. Fe_2O_3 *K. pneumniae* NPs have 65.8% of iron and 34.2% of oxygen, respectively, and Fe_2O_3 *S. aureus* NPs have 68.2% of iron and 31.8% of oxygen; the results are near from previously reported results[19,26] [Figure 7].

The greatest concentrations of Fe_2O_3 NPs were similar in size to a tiny concentration of big particles. The Fe_2O_3 NPs showed some agglomeration as well, which is typical of the synthesis of green NPs. The fact that green-synthesized NPs have a higher surface area and are very adherent to one another is what causes this aggregation.

Conclusion

We deduced from the findings of the current investigation that *K. pneumoniae* and *S. aureus* bacteria are both capable of producing Fe_2O_3 NPs extracellularly and that the size of the NPs produced by *K. pneumoniae* was smaller than those produced by *S. aureus*. Because extracellular methods are excellent candidates for creating Fe_2O_3 NPs, we advise using them to produce NPs. We also advise researching how these NPs interact with various infections in humans and animals from a pharmacological standpoint.

Financial Support and Sponsorship

Nil.

Conflicts of Interest

There are no conflicts of interest.

References

1. Chatterjee K, Sarkar S, Rao KJ, Paria S. Core/shell nanoparticles in biomedical applications. Adv Colloid Interface Sci 2014;209:8-39.
2. Dorniani D, Hussein MZ, Kura AU, Fakurazi S, Shaari AH, Ahmad Z. Preparation of Fe_3O4 magnetic nanoparticles coated with gallic acid for drug delivery. Int J Nanomed 2012;12:5745-56.
3. Prijic S, Sersa G. Magnetic nanoparticles as targeted delivery systems in oncology. Radiol Oncol 2011;45:1-16.
4. Mohammed L, Gomaa HG, Ragab D, Zhu J. Magnetic nanoparticles for environmental and biomedical applications: A review. Particuology 2017;30:1-14.
5. Khairi AW, Naji GA. The effect of silica nano particle derived from natural rice on surface roughness and wettability of high impact heat cure resin. Med J Babylon 2023;20:308-14.
6. -Sanvicens N, Marco MP. Multifunctional nanoparticles–properties and prospects for their use in human medicine. Trends Biotechnol 2008;26:425-33.
7. Sundaram PA, Augustine R, Kannan M. Extracellular biosynthesis of iron oxide nanoparticles by *Bacillus subtilis* strains isolated from rhizosphere soil. Biotechnol Bioprocess Eng 2012;17:835-40.
8. Dormann JL, Bessais L, Fiorani D. A dynamic study of small interacting particles: Superparamagnetic model and spin-glass laws. J Phys C: Solid State Phys1988;21:2015.
9. Li X, Xu H, Chen ZS, Chen G. Biosynthesis of nanoparticles by microorganisms and their applications. J Nanomater 2011;2011: 1-16.

10. Hagedorn S, Kaphammer B. Microbial biocatalysis in the generation of flavor and fragrance chemicals. Annu Rev Microbiol 1994;48:773-800.
11. Al-Zaidi JR. Methicillin resistant *Staphylococcus aureus* (MRSA) nasal carriage among health care workers in intensive care units. Med J Babylon 2014;11:749-57.
12. Baker RA, Tatum JH. Novel anthraquinones from stationary cultures of *Fusarium oxysporum*. J Ferment Bioeng 1998;85:359-61.
13. Seo WS, Lee JH, Sun X, Suzuki Y, Mann D, Liu Z, *et al*. FeCo/graphitic-shell nanocrystals as advanced magnetic-resonance-imaging and near-infrared agents. Nat Mater 2006;5:971-6.
14. Sadowski Z, Maliszewska IH, Grochowalska B, Polowczyk I, Kozlecki T. Synthesis of silver nanoparticles using microorganisms. Mater Sci Poland 2008;26:419-24.
15. Saifuddin N, Wong CW, Yasumira AA. Rapid biosynthesis of silver nanoparticles using culture supernatant of bacteria with microwave irradiation. E-J Chem 2009;6:61-70.
16. Jebur YM, Abd FG. Biosynthesis of MgO nanoparticles by using *Streptococcus* species and its antibacterial activity. Biochem Cell Arch 2021;21:2557-63.
17. Mohanasrinivasan V, Subathra Devi C, Mehra A, Prakash S, Agarwal A, Selvarajan E, *et al*. Biosynthesis of MgO nanoparticles using *Lactobacillus* sp and its activity against human leukemia cell lines HL-60. BioNanoScience 2018;8:249-53.
18. Hassan DF, Mahmood MB. Biosynthesis of iron oxide nanoparticles using *Escherichia coli*. Iraqi J Sci 2019;26:453-9.
19. Jagathesan G, Rajiv P. Biosynthesis and characterization of iron oxide nanoparticles using *Eichhornia crassipes* leaf extract and assessing their antibacterial activity. Biocatal Agric Biotechnol 2018;13:90-4.
20. Abdullah JA, Eddine LS, Abderrhmane B, Alonso-González M, Guerrero A, Romero A. Green synthesis and characterization of iron oxide nanoparticles by *Phoenix dactylifera* leaf extract and evaluation of their antioxidant activity. Sustainable Chem Pharm 2020;17:100280.
21. Takami S, Sato T, Mousavand T, Ohara S, Umetsu M, Adschiri T. Hydrothermal synthesis of surface-modified iron oxide nanoparticles. Mater Lett 2007;61:4769-72.
22. Alangari A, Alqahtani MS, Mateen A, Kalam MA, Alshememry A, Ali R, *et al*. Iron oxide nanoparticles: Preparation, characterization, and assessment of antimicrobial and anticancer activity. Adsorp Sci Technol 2022;2022:1-9.
23. Singh P, Mijakovic I. Antibacterial effect of silver nanoparticles is stronger if the production host and the targeted pathogen are closely related. Biomedicines 2022;10:628.
24. Ennas G, Musinu AN, Piccaluga G, Zedda D, Gatteschi D, Sangregorio C, *et al*. Characterization of iron oxide nanoparticles in an Fe2O3–SiO_2 composite prepared by a sol–gel method. Chem Mater 1998;10:495-502.
25. Fani M, Ghandehari F, Rezaee M. Biosynthesis of iron oxide nanoparticles by cytoplasmic extract of bacteria lactobacillus fermentum. J Med Chem Sci 2018;1:28-30.
26. Khan S, Bibi G, Dilbar S, Iqbal A, Ahmad M, Ali A, *et al*. Biosynthesis and characterization of iron oxide nanoparticles from *Mentha spicata* and screening its combating potential against *Phytophthora infestans*. Front Plant Sci 2022;13:1001499.